Electronic Supporting Information

NiII Formate Complexes with Bi- and Tridentate Nitrogen-Donor Ligands: Synthesis, Characterization, Magnetic and Thermal Properties †

Karoline Rühlig[a], Akerke Abylaikhan[a], Azar Aliabadi[b], Vladislav Kataev[b], Simon Liebing[c], Sebastian Schwalbe[c], Kai Trepte[d], Christian Ludt[c], Jens Kortus[c], Bernd Büchner[b], Tobias Rüffer[a,*], and Heinrich Lang[a]

[a)] *Technische Universität Chemnitz, Faculty of Natural Sciences, Institute of Chemistry, Inorganic Chemistry, 09107 Chemnitz, Germany.*

[b)] *IFW Dresden, Helmholtzstraße 20, 01069 Dresden, Germany.*

[c)] *TU Bergakademie Freiberg, Institute of Theoretical Physics, Leipziger Strasse 23, 09599 Freiberg, Germany.*

[d)] *TU Dresden, Institute for Theoretical Chemistry, Bergstrasse 66b, 01307 Dresden, Germany.*

Content

Elemental analysis of hygroscopic **2**	2
IR spectra of **2 – 5**	2
Extended theoretical investigations	3
Thermal decomposition characteristics of **1 – 5**	5
Crystal and structural refinement data of **2 – 5**	6
Ni–N bond distances of C_1 symmetric *mer*-$[Ni(dien)_2]^{2+}$ complex fragments	7
Comparison of structural parameters of **3@100K** and **3@293K**	9
Hydrogen bonds in the crystal structure of **5**	12

*Elemental analysis of isolated hygroscopic **2** referring to **2**·H_2O and **2**·2.5H_2O:*

Anal. Calc. for **2·2.5 H_2O** $C_8H_{31}N_6NiO_{6.5}$ (374.06): C, 25.69; H, 8.35; N, 22.47 %. Found: C, 25.99; H, 8.47; N, 22.74 %.

Chemical Formula: for **2·H_2O** $C_8H_{28}N_6NiO_5$ (347.04): C, 27.69; H, 8.13; N, 24.22 %. Found: C, 27.82; H, 8.12; N, 23.92 %.

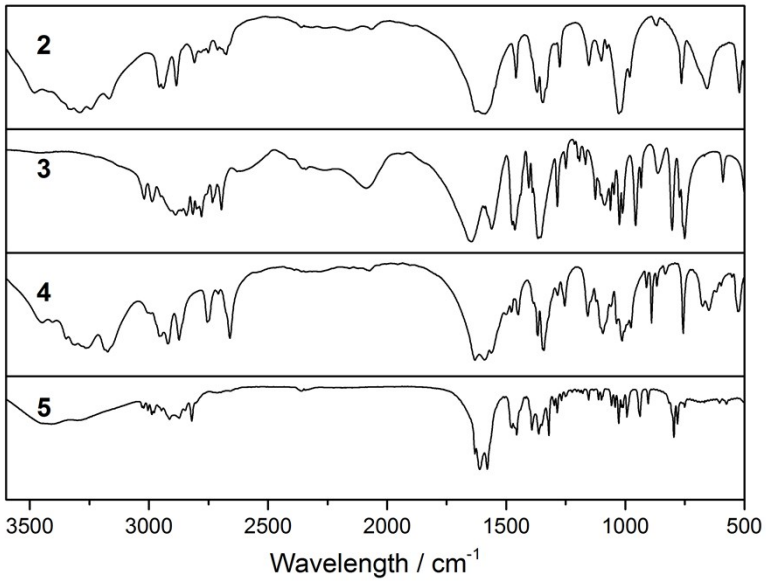

Figure S1. IR spectra of complexes **2** – **5** (KBr pellet).

Extended theoretical investigations

For further investigations, we used some additional codes, in order to validate the free molecule calculations against solid state calculations with periodic boundary conditions.

GPAW: Projector-augmented wave (PAW) calculations were performed with the GPAW code[1]

The Python code atomic simulation environment (ASE) was used to center the molecule **3A** in a (20x20x20) $Å^3$ simulation cell for all GPAW calculations. The cell size has been varied to this size to omit basis set problems, where wavefunctions do not vanish at the boundaries. Inner electrons were treated with a frozen core approach. For reasons of transferability and comparability, the same exchange-correlation potential PBE[2] has been used. Furthermore, all PAW calculations were performed spin polarized. The linear combination of atomic orbitals (LCAO) mode and finite difference (FD) mode were applied to all magnetic ground state calculations as needed for the derivation of the coupling constant *J*. All calculations were done with optimized double zeta polarized (dzp) basis sets implemented in the GPAW.

QUANTUM ESPRESSO: The code Quantum ESPRESSO[3] uses a plane wave (PW) basis set and a pseudopotential approximation employing the PAW method. A kinetic energy cutoff for wavefunctions of 90 Ry was used for all calculations. Again, the GGA-PBE exchange correlation functional has been used. For such calculations, the cell size was chosen such that there is a minimum of 10 Å of vacuum to any adjacent molecule in each direction. For PW calculations, there are no convergence problems based on basis set functions which stick out of the cell. Additional calculations involved van der Waals corrections as introduced by Grimme 46: to analyze the influence of such corrections on the geometry the and the resulting coupling constants.

CP2K: CP2K[4,5] uses a mixed planewave and gaussian basis set. For our calculations we used a DZVP basis set and again the widely used GGA-PBE functional. The IR spectra was calculated of **3A** without periodic boundary conditions centered in a box with 10 Å of vacuum in each direction. For an accurate IR spectra the initial geometry was optimized to reduce the forces to less then 0.003 eV/Å.

*Extended magnetic properties of **3***

Table S1. This is an extension of Table 6: For each calculation, the used code and the applied methods is given. LCAO = linear combination of atomic orbitals, FD = finite differences, PW = plane waves, dzp = double zeta polarized basis set, PAW = projector-augmented wave method and vdW = calculation with van der Waals corrections.

Code & Type	Basis	Molecule	Geometry	J [cm^{-1}]
GPAW, LCAO	dzp	**3.A**	unrelaxed	–16.62
GPAW, FD	dzp	**3.A**	unrelaxed	–16.68
GPAW, LCAO	dzp	**3.A**	relaxed	–7.69
QE, PAW	PW	**3.A**	unrelaxed	–16.25
QE, PAW	PW	**3.A**	relaxed	–11.03
QE, PAW	PW	**3.A**	relaxed with vdW	–10.16

Different implementations of DFT provide similar results for the coupling constant. Due to the variety of independent DFT methods, the numerical errors of our results were methodically minimized. For all codes it could be seen that reliable calculations of coupling constants require an accurate structure relaxation, otherwise the results could not be trusted. We observe the same trends for pseudopotential based (GPAW and QE) as for the all-electron calculations with the NRLMOL code.

Extended theoretical IR spectra

As already discussed in the result section (IR spectroscopy) major experimental peaks can be assigned to calculated ones via vibrational mode identification. Different basis sets are the source for shifts for differently calculated spectra.

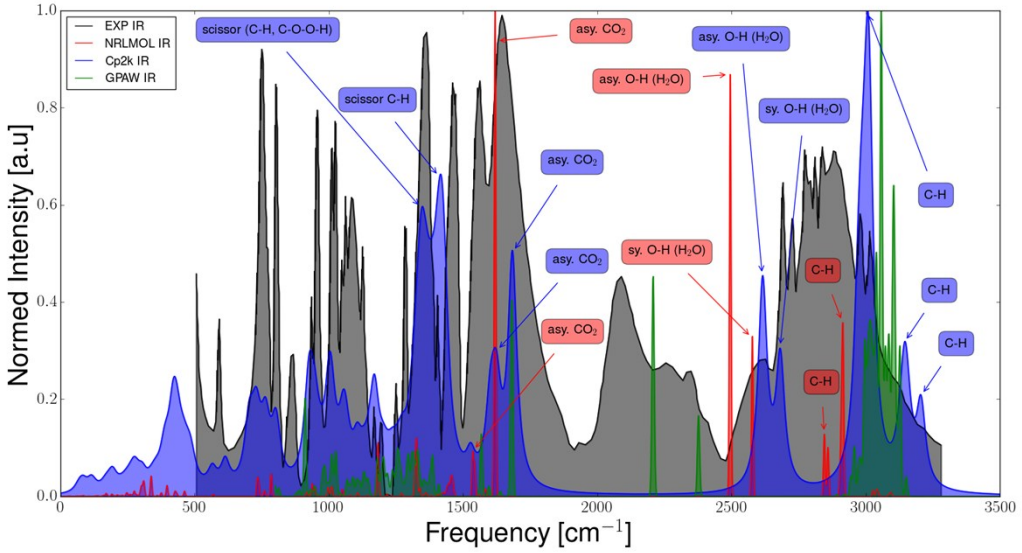

Figure S2. Experimental and calculated IR spectra of **3**. The theoretical spectra were calculated within the harmonic approximation. Intense peaks are indexed with their vibration mode.

1 J. Enkovaara, C. Rostgaard, J. J. Mortensen, J. Chen, M. Dułak, L. Ferrighi, J. Gavnholt, C. Glinsvad, V. Haikola, H. a Hansen, H. H. Kristoffersen, M. Kuisma, a H. Larsen, L. Lehtovaara, M. Ljungberg, O. Lopez-Acevedo, P. G. Moses, J. Ojanen, T. Olsen, V. Petzold, N. a Romero, J. Stausholm-Møller, M. Strange, G. a Tritsaris, M. Vanin, M. Walter, B. Hammer, H. Häkkinen, G. K. H. Madsen, R. M. Nieminen, J. K. Nørskov, M. Puska, T. T. Rantala, J. Schiøtz, K. S. Thygesen and K. W. Jacobsen, *J. Phys. Condens. Matter*, 2010, **22**, 253202.

2 J. P. Perdew, K. Burke and M. Ernzerhof, *Phys. Rev. Lett.*, 1996, **77**, 3865.

3 P. Giannozzi, S. Baroni, N. Bonini, M. Calandra, R. Car, C. Cavazzoni, D. Ceresoli, G. L. Chiarotti, M. Cococcioni, I. Dabo, A. Dal Corso, S. de Gironcoli, S. Fabris, G. Fratesi, R. Gebauer, U. Gerstmann, C. Gougoussis, A. Kokalj, M. Lazzeri, L. Martin-Samos, N. Marzari, F. Mauri, R. Mazzarello, S. Paolini, A. Pasquarello, L. Paulatto, C. Sbraccia, S. Scandolo, G. Sclauzero, A. P. Seitsonen, A. Smogunov, P. Umari and R. M. Wentzcovitch, *J. Phys. Condens. Matter*, 2009, **21**, 395502.

4 M. Krack and M. Parrinello, *NIC Ser.*, 2004, **25**, 29.

5 J. VandeVondele, M. Krack, F. Mohamed, M. Parrinello, T. Chassaing and J. Hutter, *Comput. Phys. Commun.*, 2005, **167**, 103.

Table S2. Thermal decomposition characteristics of **1** – **5**.

Compound	Temperature range	Δm (%)	Calculation of content of expelled groups[a)]
1	110–175	–20.52 %	
	175–280	–47.13 %	
		∑ –67.7 %	–2 O_2CH; –2 H_2O = 68.23 %
	280–500	+1.54 %	
2	40–130	–9.64 %	
	150–355	–71.86 %	
		∑ –81.5 %	–¾ EtOH, 3 en, –2 O_2CH, –MeOH = 79.86 %
	355–500	+0.67 %	
3	40–270	–78.25 %	–2 tmeda, –4 O_2CH, –H_2O = 78.57 %
	270–500	+2.45 %	
4	190–320	–81.27 %	
	320–500	–2.28 %	
		∑ –83.55 %	–2 dta, –2 O_2CH = 83.75 %
5	90 – 120	–1%	
	150–230	–80.16 %	
		= 81.16 %	– 2pmdta, –4 O_2CH, –1 H_2O = 88.62 %
	230–500	+1.0 %	

Table S3. Crystal and structural refinement data of **2** – **5**.

Compound	**2**	**3@100K**	**3@293K**	**4**	**5**
Empirical Formula	$C_{38}H_{122}N_{24}Ni_4O_{19}$	$C_{16}H_{38}N_4Ni_2O_9$	$C_{16}H_{38}N_4Ni_2O_9$	$C_{10}H_{28}N_6NiO_4$	$C_{22}H_{52}N_6Ni_2O_9$
Formula weight (g/mol)	1454.43	547.92	547.92	355.09	662.11
Temperature (K)	200	100	293	110	110
Crystal system	monoclinic	monoclinic	monoclinic	monoclinic	monoclinic
Space group	$P2_1/c$	$C2/c$	$C2/c$	$P2_1/c$	Cc
a (Å)	9.7670(4)	26.9488(11)	27.1365(6)	13.2477(5)	30.8174(7)
b (Å)	15.3025(5)	13.7861(5)	13.9455(2)	8.7413(3)	8.5618(4)
c (Å)	12.9080(5)	27.4426(14)	27.7677(6)	13.7152(5)	13.1881(6)
β (°):	111.908(5)	108.680(5)	108.481(2)	92.087(3)	119.006(3)
V (Å^3)	1789.90(13)	9658.4(8)	9966.3(4)	1587.2(1)	3043.2(2)
Radiation source	Cu K_α	Mo K_α	Cu K_α	Mo K_α	Mo K_α
λ (Å)	1.54184	0.71073	1.54184	0.71073	0.71073
Z	1	16	16	4	4
D_{calc} (g/cm^3)	1.349	1.507	1.461	1.486	1.443
μ (mm^{-1})	1.814	1.610	2.314	1.248	1.291
F(000)	782	4640	4640	760	1416
Reflections collected	14254	23504	77514	6343	10743
Reflections unique	5911	8424	16923	2801	4941
R_{int}[a]	0.0510	0.0450	0.0212	0.0195	0.0309
Index ranges	$-11 \le h \le 11$	$-32 \le h \le 31$	$-32 \le h \le 32$	$-15 \le h \le 15$	$-35 \le h \le 36$
	$-14 \le k \le 17$	$-16 \le k \le 16$	$-16 \le k \le 16$	$-10 \le k \le 10$	$-10 \le k \le 9$
	$-14 \le l \le 14$	$-31 \le l \le 32$	$-33 \le l \le 33$	$-16 \le l \le 16$	$-15 \le l \le 15$
$\theta_{min.}/\theta_{max.}$(°)	4.689/ 62.492	3.057/24.998	3.695/66.999	2.972/24.999	3.023/24.996
Data/Restrains/Parameters	5911/186/256	8424/20/585	16923/36/580	2801/10/230	4941/5/360
Goodness-of-fit on F^2 [b]	1.018	1.037	0.958	1.050	1.030
R_1 / wR_2 [$I > 2\sigma(I)$][c]	0.0691/0.2240	0.0369/0.0843	0.0395/0.1049	0.0345/0.0772	0.0259/0.0575
R_1 / wR_2 [all data]	0.0952/0.2365	0.0501/0.0906	0.0511/0.1081	0.0389/0.0792	0.0280/ 0.0587
Largest diff. peak/hole [eÅ^{-3}]	0.951/–0.619	0.579/–0.450	0.282/–0.442	0.902/–0.433	0.273/–0.256

[a] $R_{int} = \sum|F_o^2 - F_o^2(mean)|/\sum F_o^2$, where $F_o^2(mean)$ is the average intensity of symmetry equivalent diffraction.
[b] $S = [\sum w(F_o^2 - F_c^2)^2]/(n-p)^{1/2}$, where n = number of reflections, p = number of parameters.
[c] $R1 = [\sum(||F_o| - |F_c|)/\sum|F_o|]$, $wR2 = [\sum w(F_o^2 - F_c^2)^2)/\sum w(F_o^4)]^{1/2}$.

Ni–N bond distances of C_1 symmetric *mer*-$[Ni(dien)_2]^{2+}$ complex fragments: The shortest Ni1−N bonds are formed between the secondary amino N donor atoms (*d*(Ni1−N2/Ni1−N5) = 2.089(2)/2.082(2) Å), group I. One of the primary amino N donor atoms are bonded by a significantly longer Ni1−N distance when compared with group I, cf. *d*(Ni1−N1/Ni1−N6) = 2.116(2)/2.130(2) Å, group II. The remaining primary amino N donor atoms of both dien ligands are then bonded by even longer Ni1−N distances when compared with group II, cf. *d*(Ni1−N3/Ni1−N4) = 2.142(2)/2.143(2) Å, group III. For related *mer*-$[Ni(dien)_2]^{2+}$ complex fragments this phenomena has been sometimes acknowledged [6,7] and it seems that it is of broader validity for $[M(dien)_2]^{2+}$ fragments (M = Zn, Co, Cu),[7] although its origin remains unclear. The possibility that this phenomena is originated by different types and strengths of intermolecular hydrogen bonds, in which the $[Ni(dien)_2]^{2+}$ complex fragment of **4** is involved in the solid state, can be ruled out. For a further discussion involving other crystallographically characterized compounds comprising C_1 symmetric *mer*-$[Ni(dien)_2]^{2+}$ complex fragments see below Scheme S1 and the accompanying discussion.

6 J. Černák, J. Paharová, J. Skoršepa and W. Massa, *Zeitschrift für Anorg. und Allg. Chemie*, 2002, **628**, 344.

7 V. Rodriguez, J. M. Gutierrez-Zorilla, P. Vitoria, A. Luque, P. Roman and M. Martinez-Ripoll, *Inorg. Chim. Acta*, 1999, **290**, 57.

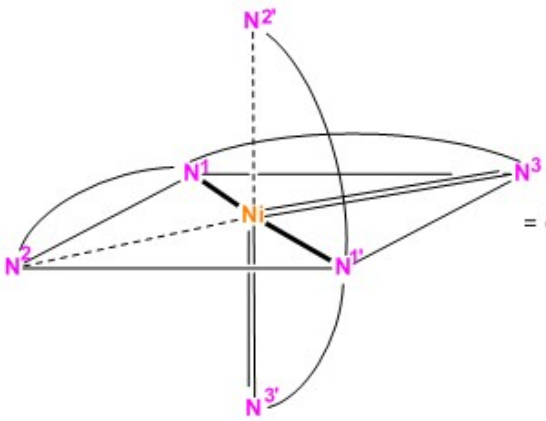

= C_1 symmetric $[Ni(dien)_2]^{2+}$ complex fragments

CSD Refcode	Formula	Bond distances (Å)		
		Ni–N1/Ni–N1'	Ni–N2/Ni–N2'	Ni–N3/Ni–N3'
AEAMNI11	$[Ni(dien)_2]Cl_2 \cdot H_2O$	2.081/2.082	2.125/2.149	2.159/2.165
BIPPEX	$[Ni(dien)_2][Ni(As_3S_3)_2]$	2.063/2.077	2.129/2.107	2.193/2.118
CEYROO	$[Ni(dien)_2][CdCl_4] \cdot H_2O$	2.076/2.091	2.137/2.119	2.150/2.167
HOKXEK	$[Ni(dien)_2][Ni(CN)_4] \cdot H_2O$	2.070/2.091	2.148/2.147	2.186/2.163
IHUGEX	$[Ni(dien)_2](NO_3)_2$	2.085/2.087	2.133/2.153	2.160/2.145
NOHZUG	$[Ni(dien)_2][Ni(S_2C_4N_2)_2]$	2.066/2.070	2.149/2.145	2.164/2.150
ODIWAZ	$[Ni(dien)_2][Pd(CN)_4]$	2.076/2.072	2.130/2.122	2.162/2.166
TAKYAG	$[Ni(dien)_2][Ni(CN)_4]$	2.064/2.073	2.136/2.121	2.180/2.185
XAKBOB	$[Ni(dien)_2][Ni(CN)_4] \cdot 2H_2O$	2.057/2.074	2.138/2.140	2.187/2.154

Scheme S1. Ni–N bond distances of C_1 symmetric *mer*-$[Ni(dien)_2]^{2+}$ complex fragments.

Brief discussion: Scheme S1 summarizes on selected entries within the Cambridge Structural Database, that is, not all C_1 symmetric *mer*-$[Ni(dien)_2]^{2+}$ complex fragments have been acknowledged here. Namely, corresponding entries with comparatively small counter ions were considered. Despite this, entries in Scheme S1 display that the in the manuscript discussed phenomena of different Ni–N bond lengths has been observed more frequently, if not always. All complexes considered in Scheme S1 exhibits in the solid state intermolecular hydrogen bonds between the N–H donor functions of the $[Ni(dien)_2]^{2+}$ complex fragments and corresponding acceptor functionalities (A). Without illustrating them in detail it seems extremely likely that the overall features of the intermolecular hydrogen bonds (1D chains, 2D layers, 3D network; number of individual N–H···A interactions and their geometrical features) differ from entry to entry. Consequently, the expected different hydrogen bonding motifs of the $[Ni(dien)_2]^{2+}$ complex fragments in the solid state may not explain the phenomena of the different Ni-N bond distances, which should be thus addressed to an "intrinsic" property of the complex fragment itself.

*Comparison of structural parameters of **3@100K** and **3@293K***: As early as in 1961 Becka and Cruickshank described the phenomena that uncorrected bond lengths appear virtually larger with decreasing temperature.[11] Such a finding has been made since then several times and is generally accepted.[12] According to Becka and Cruickshank[11] it is possible to apply motional corrections by which bond lengths were shown to become independent from the measurement temperatures.[12] In order to decide whether a difference in bond lengths (Δl) is significant or not, Cruickshank introduced the so-called 3σ criteria.[13] Thus, a difference Δl counts as significant when its value is larger compared to the value of 3σ, whereby 3σ is derived from the standard deviations of bond lengths or angles under investigation.[13]

The question arises whether a decrease of (always uncorrected) bond lengths with decreasing temperature might be attributable to a certain physical property of the material under investigation. Indeed, concrete examples have been already reported. Spin crossover complexes, especially Fe^{II}-containing ones, exhibit at lower measurement temperatures significantly decreased Fe–D (D = donor atom) bond lengths, when compared with values determined at room temperature.[14] In accordance with the independently determined spin crossover behavior, the decrease in bond lengths is attributed to the presence of low-spin/high-spin complexes at lower/higher temperatures.[14] Furthermore, Benbellat *et al*. did describe for the binuclear Co^{II} paddlewheel complex $[Co_2(PhCO_2)_4(L)_2]$ a significant shortening of the $Co^{II}\cdots Co^{II}$ distance with decreasing temperature, while other bond distances increase slightly.[15] This temperature dependence of the molecular structure evidenced that "the magnetism of this complex can be interpreted in terms of weak metal-metal interaction between the two Co^{II} ions".[15] Thus, through-bridge magnetic superexchange pathways along the carboxylate ligands could be most likely ruled out for this d^7–d^7 dimer, although related d^9–d^9 dimers feature them.[15] Here reported **3** can be described as a d^8–d^8 dimer, whereby the d^8 ions are bridged by one μ-H_2O and two μ-O_2CH carboxylate ligands, cf. Fig. 4 in the manuscript. Variable temperature measurements of **3** were thus performed with the aim to verify whether bond lengths will show temperature dependence by which an independent indication of magnetic superexchange pathways might be possible.

Table S4. Selected bond distances (Å) and angles (°) of **3A/3B@100K** and of **3A/3B@293K**.

Bond lenghts					
	3@100K 3A/3B	**3@293K 3A/3B**		**3@100K 3A/3B**	**3@293K 3A/3B**
Ni1–N1	2.156(2)/2.161(2)	2.193(2)/2.166(2)	C1–O1	1.246(3)/1.246(3)	1.242(3)/1.234(3)
Ni1–N2	2.152(2)/2.148(2)	2.160(2)/2.152(2)	C1–O2	1.249(3)/1.252(3)	1.228(3)/1.242(3)
Ni1–O1	2.0369(19)/2.035(2)	2.0415(17)/2.0319(19)	C2–O3	1.249(3)/1.241(3)	1.244(3)/1.230(3)
Ni1–O3	2.0325(19)/2.036(2)	2.0398(17)/2.0458(19)	C2–O4	1.251(3)/1.252(3)	1.234(3)/1.239(3)
Ni1–O5	2.0850(19)/2.073(2)	2.0953(17)/2.071(2)	C3–O5	1.248(3)/1.248(4)	1.241(4)/1.241(4)
Ni1–O9	2.1115(19)/2.116(2)	2.0993(18)/2.1200(16)	C3–O6	1.228(3)/1.242(4)	1.232(4)/1.226(4)
Ni2–N3	2.155(2)/2.165(2)	2.1522(19)/2.175(3)	C4–O7	1.256(3)/1.251(4)	1.251(3)/1.242(4)
Ni2–N4	2.186(2)/2.174(2)	2.164(2)/2.182(2)	C4–O8	1.237(3)/1.244(4)	1.236(4)/1.219(5)
Ni2–O2	2.0368(19)/2.0345(19)	2.0385(18)/2.0433(19)	O9···O6	2.537(3)/2.566(3)	2.586(3)/2.579(4)
Ni2–O4	2.0414(19)/2.0361(19)	2.0353(18)/2.0287(18)	O9···O8	2.579(3)/2.575(3)	2.545(3)/2.579(4)
Ni2–O7	2.0957(19)/2.0910(19)	2.083(2)/2.0857(19)	Ni1···Ni2	3.5993(5)/3.6005(5)	3.6058(8)/3.6086(8)
Ni2–O9	2.091(2)/2.102(2)	2.1194(15)/2.1170(19)			
Bond angles					
N1–Ni1–N2	84.65(8)/84.64(9)	83.77(9)/84.32(9)	N3–Ni2–N4	84.13(9)/84.41(9)	84.35(8)/84.39(10)
N1–Ni1–O1	90.69(8)/90.40(8)	90.76(8)/90.25(9)	N3–Ni2–O2	89.41(8)/89.84(9)	88.75(8)/89.55(9)
N1–Ni1–O3	172.2(1)/172.1(1)	171.60(8)/171.95(8)	N3–Ni2–O4	86.84(8)/88.78(9)	88.59(8)/88.65(9)
N1–Ni1–O5	88.94(8)/89.10(8)	88.71(8)/89.48(9)	N3–Ni2–O7	90.88(8)/87.55(9)	90.75(8)/87.95(9)
N1–Ni1–O9	94.65(8)/95.69(9)	95.58(8)/95.88(7)	N3–Ni2–O9	178.8(1)/178.2(1)	178.67(8)/178.31(8)
N2–Ni1–O1	88.01(8)/87.96(8)	87.23(8)/88.92(8)	N4–Ni2–O2	171.4(1)/172.3(1)	172.36(8)/172.71(8)
N2–Ni1–O3	88.68(8)/88.52(8)	89.68(8)/88.25(8)	N4–Ni2–O4	90.59(8)/91.10(8)	90.71(8)/90.51(8)
N2–Ni1–O5	90.87(8)/90.41(9)	90.86(8)/90.36(9)	N4–Ni2–O7	88.65(8)/88.48(8)	88.99(9)/88.80(8)
N2–Ni1–O9	178.0(1)/178.8(1)	178.85(8)/179.30(9)	N4–Ni2–O9	95.48(8)/94.31(9)	95.05(7)/95.06(8)
O1–Ni1–O3	93.17(8)/93.33(8)	94.18(8)/92.70(9)	O2–Ni2–O4	94.67(8)/93.91(8)	92.40(8)/93.40(8)
O1–Ni1–O5	178.8(1)/178.3(1)	178.06(8)/179.25(8)	O2–Ni2–O7	85.82(8)/86.15(8)	87.81(9)/86.94(9)
O1–Ni1–O9	90.13(8)/90.93(8)	91.83(7)/90.42(7)	O2–Ni2–O9	91.09(8)/91.32(8)	91.91(7)/90.89(7)
O3–Ni1–O5	87.07(8)/86.98(8)	86.13(8)/87.48(9)	O4–Ni2–O7	177.7(1)/176.3(1)	179.31(8)/176.59(9)
O3–Ni1–O9	92.14(8)/91.22(8)	91.05(7)/91.59(7)	O4–Ni2–O9	92.01(8)/92.55(9)	90.23(7)/92.95(7)
O5–Ni1–O9	90.99(8)/90.70(8)	90.08(7)/90.30(8)	O7–Ni2–O9	90.27(8)/91.11(9)	90.42(7)/90.44(8)
O1–C1–O2	129.7(3)/129.7(3)	130.1(2)/130.0(3)	O5–C3–O6	129.6(3)/128.4(3)	128.9(3)/128.6(3)
O3–C2–O4	129.4(3)/129.7(3)	129.8(2)/130.0(2)	O7–C4–O8	129.2(3)/127.9(3)	127.6(3)/129.1(3)
O9–H1···O6	174(3)/169(4)	152/150	O9–H2···O8	166(3)/166(4)	151/150
Ni1–O9–Ni2	117.9(1)/117.2(1)	117.51(8)/116.81(8)			

The averaged Ni···Ni distance of **3@100K** is with 3.5999(7) Å slightly, but significantly, shorter when compared to the value of **3@293K** (3.6072(11) Å), although it can be ruled out that that the magnetism of **3** is governed by metal-metal interactions. A comparison of the averaged values of the Ni–O_{H2O} bond lengths reveals, that the ones including Ni1/Ni3 (**3A**/**3B**, Table S4) appear longer at 100 K (100 K: average = 2.1137(28) Å; 293 K: 2.10965(24) Å), whereas the one including Ni2/Ni4 are shortened (100 K: average = 2.0965(28) Å; 293 K: 2.1182(24) Å). Noticeable, the Ni–O_{H2O}–Ni bond angles show no significant differences. Furthermore, all bond lengths and angles in which the two μ-O_2CH carboxylate ligands are involved are not affected by the temperature influence. In this context a further variable temperature study of a type **3-Ni$_2$** complex with R = CF_3[10] should be mentioned. Independently, the molecular structure was determined at 295 K[8,14] and at 123 K.[9,10] As observed for **3**, the Ni···Ni distance of this complex decreases with decreasing temperature (295 K: 3.676(3) Å; 123 K:

3.647(3) Å), which is accompanied by the shortening of one Ni–O_{H2O} bond while the second one remains unaffected by temperature influence. Other bonds do not show significant differences within the 3σ criteria. As bond lengths of **3@100K**, when compared with related ones of **3@293K**, due only sparingly show significant differences, an assignment of the magnetic superexchange coupling path is not reliably possible. However, these observations indicate that the two d^8 ions may not exclusively interact magnetically with each other via the μ-H_2O ligand but via the two μ-O_2CH carboxylate ligands as well.

8 Within the Cambrige Structural Database (CSD), Conquest Version 1.18, 93 entries could be identified.

9 U. Turpeinen, M. Ahlgren and R. Hämäläinen, Finn. Chem. Lett., 1977, 246.

10 (a) U. Turpeinen and M. Ahlgren, Acta Crystallogr., Sect. B., 1982, 38, 276. (b) M. Nieger, CSD Private Communication: BAXLUH01, 2003.

11 L. N. Becka and D. W. J. Cruickshank, Acta Cryst., 1961, 14, 1092.

12 J. D. Dunitz, V. Schomaker and K. N. Trueblood, J. Phys. Chem., 1988, 92, 856.

13 D. W. J. Cruickshank, Acta Cryst., 1949, 2, 65.

14 (a) S. Mossin, B. L. Tran, D. Adhikari, M. Pink, F. W. Heinemann, J. Sutter, R. K. Szilagyi, K. Meyer and D. J. Mindiola, J. Am. Chem. Soc., 2012, 134, 13651. (b) S. Heider, H. Petzold, G. Chastanet, S. Schlamp, T. Rüffer, B. Weber and J.-F. Létard, Dalton Trans., 2013, 42, 8575.

15 N. Benbellat, K. S. Gavrilenko, Y. Le Gal, O. Cador, S. Golhen, A. Gouasmia, J.-M. Fabre and L. Ouahab, Inorg. Chem., 2006, 45, 10440.

Hydrogen bonds in the crystal structure of ***5***: Most likely, all in the manuscript mentioned differences between **5A** and 5**B** can be explained by the interaction of exclusively **5A** with one water molecule by means of hydrogen bonds (Fig. S3 and Table S5). Due to them, 1D chains are formed along the crystallographic *b*-axis. The water molecule interacts thereby with both an oxygen atom of the κ^2O,O'- and κO-bonded formate ligand of **5A** and has thus impact on the C–O and Ni–O, but not on the Ni–N bonds of **5A**.

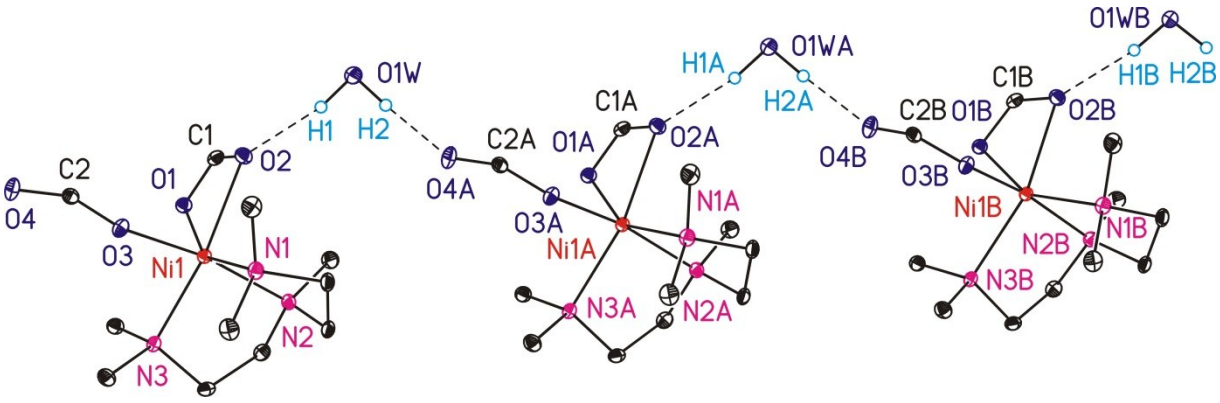

Fig. S3 Illustration of a representative part of one selected 1D polymeric chain formed of **5A** and H_2O in the solid state. All *carbon*-bonded hydrogen atoms are omitted for clarity. Intermolecular hydrogen bonds are indicated by dashed lines. Symmetry operations: (A) *x*, 1–*y*, *z*; (B) *x*, 2–*y*, *z*.

Table S5. Bond lengths (Å) and angles (°) of the intermolecular hydrogen bonds formed between **5A** and H_2O.

	5A[a)]		
D–H···A	D···A	D–H···A	line code[b)]
O1W–H1···O2	2.850(6)	164(6)	- - - - -
O1W–H2···O4A	2.759(4)	177(6)	- - - - -

[a)] Symmetry operations: (A) *x*, 1–*y*, *z*.